San Jose State University
SJSU ScholarWorks

Faculty Publications | Electrical Engineering Department

5-1-2000

Multilevel Coded Modulation for Unequal Error Protection and Multistage Decoding—Part II: Asymmetric Constellations

Motohiko Isaka
University of Tokyo

Marc P. C. Fossorier
University of Hawaii at Manoa

Robert H. Morelos-Zaragoza
LSI Logic Corporation, robert.morelos-zaragoza@sjsu.edu

Shu Lin
University of Hawaii at Manoa

Hideki Imai
University of Tokyo

Follow this and additional works at: http://scholarworks.sjsu.edu/ee_pub

Part of the Electrical and Computer Engineering Commons

Recommended Citation

Isaka, Motohiko; Fossorier, Marc P. C.; Morelos-Zaragoza, Robert H.; Lin, Shu; and Imai, Hideki, "Multilevel Coded Modulation for Unequal Error Protection and Multistage Decoding—Part II: Asymmetric Constellations" (2000). *Faculty Publications.* Paper 15.
http://scholarworks.sjsu.edu/ee_pub/15

This Article is brought to you for free and open access by the Electrical Engineering Department at SJSU ScholarWorks. It has been accepted for inclusion in Faculty Publications by an authorized administrator of SJSU ScholarWorks. For more information, please contact Library-scholarworks-group@sjsu.edu.

Multilevel Coded Modulation for Unequal Error Protection and Multistage Decoding—Part II: Asymmetric Constellations

Motohiko Isaka, *Member, IEEE*, Marc P. C. Fossorier, *Member, IEEE*, Robert H. Morelos-Zaragoza, *Senior Member, IEEE*, Shu Lin, *Fellow, IEEE*, and Hideki Imai, *Fellow, IEEE*

***Abstract*—In this paper, multilevel coded asymmetric modulation with multistage decoding and unequal error protection (UEP) is discussed. These results further emphasize the fact that unconventional signal set partitionings are more promising than traditional (Ungerboeck-type) partitionings, to achieve UEP capabilities with multilevel coding and multistage decoding. Three types of unconventional partitionings are analyzed for asymmetric 8-PSK and 16-QAM constellations over the additive white Gaussian noise channel to introduce design guidelines. Generalizations to other PSK and QAM type constellations follow the same lines. Upper bounds on the bit-error probability based on union bound arguments are first derived. In some cases, these bounds become loose due to the large overlappings of decision regions associated with asymmetric constellations and unconventional partitionings. To overcome this problem, simpler and tighter approximated bounds are derived. Based on these bounds, it is shown that additional refinements can be achieved in the construction of multilevel UEP codes, by introducing asymmetries in PSK and QAM signal constellations.**

***Index Terms*—Asymmetric constellations, multilevel coded modulation, multistage decoding, unequal error protection, union bound.**

I. Introduction

UNCONVENTIONAL signal set partitionings are a good approach to achieve *unequal error protection* (UEP) capabilities in multilevel coded modulation and multistage decoding [1], as shown in the companion paper [2]. In general, UEP channel coding should be designed based on the characteristics of the source encoder output, with respect to the proportion and the desired quality of each bit stream. This motivates the use of nonuniform (asymmetric) signal constellations together with unconventional partitionings [3] to obtain additional freedom in the code construction.

Previous work on coded modulation for UEP with asymmetric constellations has been presented in [3]–[5], all for the additive white Gaussian noise (AWGN) channel, and in [6] and [7] for the Rayleigh/Rician fading channels. Multilevel codes were designed based on minimum squared Euclidean distance (SED) for the AWGN channel [3], and by minimum symbol and product distance for the Rayleigh fading channel [6], and computer simulations at relatively high bit-error rates (BER's). However, asymptotic evaluations based on distance parameters alone are insufficient for designing multilevel codes with multistage decoding, since the multiple representations of signal labels affect the error performance significantly at practical BER. Signal constellations named "32-diamond constellation" have been designed based on cutoff rate arguments for Rayleigh/Rician fading channels in [7]. However, this approach only deals with limited cases, and cutoff rate arguments do not predict the code performance precisely in many situations. The fact that no general theoretical analysis on the bit-error performance has been derived for multilevel codes has resulted in somewhat *ad hoc* code constructions (although in [5] an upper bound for trellis codes with maximum-likelihood decoding is presented). Therefore, a systematic approach for the construction of multilevel UEP codes is desired.

In this paper, multilevel coded asymmetric modulations with multistage decoding and UEP capabilities are discussed to obtain additional refinements in the matched design of source-channel coding systems. Three unconventional set partitionings are applied to asymmetric 8-PSK constellations and their error performance is discussed. Upper bounds on the bit-error probability, when linear block component codes are used over the AWGN channel, are derived by extending union bound arguments introduced in [2], [8], and [10] to asymmetric PSK constellations.

In deriving the pairwise-error probabilities contributing to the corresponding union bounds for multistage decoding of multilevel coded modulation schemes, two general cases are explicitly distinguished and applied in this paper. In the first case, each pair of code sequences considered in the union

Paper approved by J. Huber, the Editor for Coding and Coded Modulation of the IEEE Communications Society. Manuscript received October 8, 1998; revised March 30, 1999 and August 2, 1999. This work was supported in part by the TAO (Telecommunications Advancement Organization of Japan) International Collaborative Research Grant 8048, the National Science Foundation under Grant CCR-97-32959, and by LSI Logic Corporation. This paper was presented in part at the IEEE International Symposium on Information Theory (ISIT'98), Cambridge, MA, August 1998, and at the IEEE Global Telecommunications Conference (GLOBECOM'98), Sydney, Australia, November 1998.

M. Isaka and H. Imai are with the Institute of Industrial Science, University of Tokyo, Tokyo 1068558, Japan (e-mail: isaka@imailab.iis.u-tokyo.ac.jp).

M. P. C. Fossorier is with the Department of Electrical Engineering, University of Hawaii at Manoa, Honolulu, HI 96822 USA.

R. H. Morelos-Zaragoza was with LSI Logic Corporation, Milpitas, CA 95035-7451 USA. He is now with the Advanced Telecommunications Laboratory, SONY Computer Science Laboratories, Inc., Tokyo 141-0022, Japan.

S. Lin was with the Department of Electrical Engineering, University of Hawaii at Manoa, Honolulu, HI 96822 USA. He is now with the Department of Electrical and Computer Engineering, University of California at Davis, Davis, CA 95616-5294 USA.

Publisher Item Identifier S 0090-6778(00)04017-4.

0090–6778/00$10.00 © 2000 IEEE

bound, and representing two codewords which differ in w positions defines a distinct $2w$-dimensional decision region. These $2w$-dimensional decision regions simply correspond to the underlying two-dimensional constellation, replicated in w orthogonal dimensions, so that Pythagoras' theorem holds. This method applies to conventional Ungerboeck-type partitioning [9], as shown in [2] and [10]. However, for many unconventional partitionings (possibly together with asymmetric constellations), different pairs of code sequences considered in the union bound share the same decision regions, so that Pythagoras' theorem no longer holds. In this case, the line joining the code sequences of each pair considered in the $2w$-dimensional Euclidean space is no longer always orthogonal to the decision region considered by the decoder. As a result, the distance between the code sequence considered and the corresponding decision region is no longer always obtained from independent contributions of the symbols composing this code sequence. A second approach in evaluating the pairwise-error probability is therefore necessary, as presented in [2] although this case has not been explicitly discriminated.

It is observed that, as the distribution of nearest neighbors depends on the asymmetries, the union bound becomes loose in some cases, because of the important overlappings of decision regions. As a remedy, a tighter and simpler approximated upper bound is derived, by considering the asymmetries and corresponding equivalent numbers of nearest neighbors. This new bound is based on Pythagoras' theorem and constitutes only an approximation for many unconventional partitionings.

The same set partitioning strategies are also applied to 16-QAM constellations. It is shown that the extensions of the analytical methods developed for 8-PSK allow in many cases to derive tight bounds on the bit-error probability associated with QAM signaling. In some cases, however, a second improvement to the union bound is required. This is due to the fact that, for some unconventional partitionings, overlappings of error regions defined from the union bound may correspond to correct decisions.

Based on these tight analytical bounds, it is shown that additional refinements in choosing the number of UEP levels, and the error performances associated with each level, can be accomplished with asymmetric constellations.

The rest of the paper is organized as follows: In Section II, asymmetric 8-PSK and 16-QAM signal constellations in multilevel coded modulation for multistage decoding and UEP are introduced. Upper bounds on bit-error probability based on union bound arguments and tighter approximations are derived for three types of partitioning for asymmetric 8-PSK in Section III. In Section IV, the error performances for asymmetric 16-QAM with the three unconventional partitioning methods are derived. Finally, conclusions on this work are given in Section V.

II. Unconventional Set Partitionings of Asymetric Constellations for UEP

A. Set Partitionings

We consider three types of unconventional partitionings, originally proposed in [2] and [8] for symmetric PSK (and QAM) constellations, to provide UEP capabilities with asymmetric modulations in this paper. In *block partitioning* [2], signal points in a subset are contained in disjoint half planes at each level. It can be regarded as an opposite approach to Ungerboeck partitioning, in which the number of nearest neighbors is minimized at the expense of intra-set distance. As a result, UEP capabilities are easily achieved by using more powerful component codes at the first levels of partitioning. This approach is suitable for L levels of error protection with the same levels of partitioning (2^L-ary signal constellations). On the other hand, *hybrid-type partitionings* take the advantages of both partitioning methods to give $l(1 < l < L)$-levels of error protection. Two partitionings are considered. Direct hybrid or *hybrid-I partitioning*[1] [2] is obtained by applying block partitioning to the first $(l-1)$ index levels, followed by $(L-l+1)$ levels of Ungerboeck partitioning, with $2 \leq l \leq L$. This can be interpreted as enhancing the quality of the least important bits by Ungerboeck partitioning once all other $(l-1)$ levels have been designed based on block partitioning. Mixed hybrid or *hybrid-II partitioning* can be considered as another strategy to trade off the performance of lower index levels for an increase in the proportion of most important bits (MIB). The partitioning is done such that, at lower index levels, some signal points are grouped as in Ungerboeck partitioning. Note that it is possible to mix these *hybrid-type* approaches in one constellation, by applying the hybrid-I partitioning in higher index levels and the hybrid-II partitioning in lower index levels, although this extension is not treated in this paper. These three partitionings are depicted in Fig. 2 for an asymmetric 8-PSK constellation. The set partitionings are represented in the figures in such a way that, at first partitioning level, signal points are partitioned by color (black and white) and at the second level by symbols (square and circle).

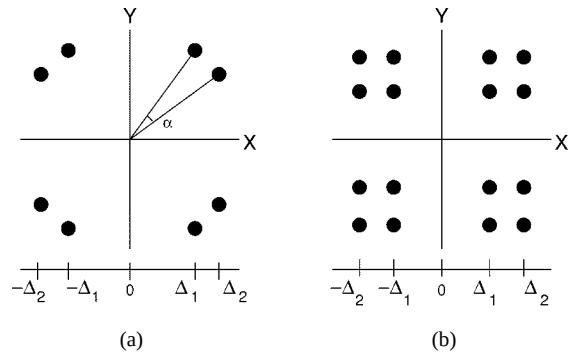

Fig. 1. Nonuniform constellations: (a) 8-PSK and (b) 16-QAM.

B. Asymmetric 8-PSK and 16-QAM Constellations

In Sections III and IV, the unconventional partitionings described above are extended to asymmetric 8-PSK and 16-QAM constellations. The 8-PSK constellation of interest in this paper is depicted in Fig. 1(a). This eight signal point constellation can be viewed as the augmentation of a pair of points in a quadrant by a $90 \cdot j\,(j = 1, 2, 3)\,^\circ$ phase rotated version of itself [11].

Let α (degrees) be the angle between two signal points in a quadrant of an 8-PSK signal constellation, where α ranges from

[1]Since another hybrid-type partitioning is considered, "hybrid" in Part I [2] is referred to as "hybrid-I" in this paper.

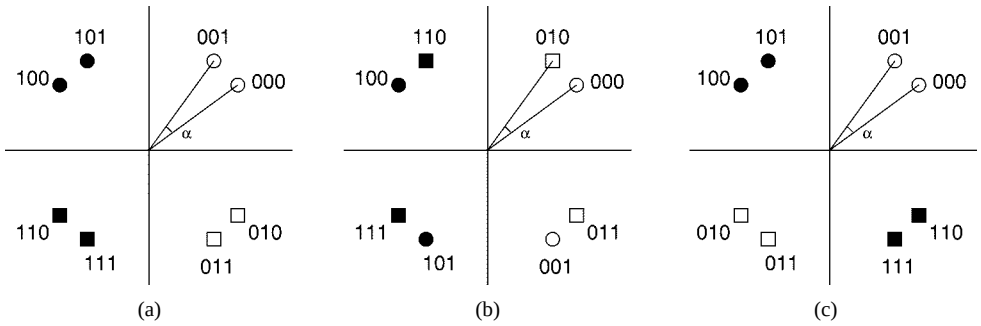

Fig. 2. Asymmetric 8-PSK constellation with: (a) block partitioning; (b) hybrid-I partitioning; (c) hybrid-II partitioning.

TABLE I
LIST OF UNCONVENTIONAL PARTITIONINGS FOR ASYMMETRIC 8-PSK MODULATIONS

Partitioning	N_1	N_2	N_3	δ_1^2	δ_2^2	δ_3^2
Block	0.5	0.5	1	$4\sin^2(\frac{90-\alpha}{360}\pi)$	$4\sin^2(\frac{90-\alpha}{360}\pi)$	$4\sin^2(\frac{\alpha}{360}\pi)$
Hybrid-I (a)	0.5	1	1	$4\sin^2(\frac{90-\alpha}{360}\pi)$	$4\sin^2(\frac{\alpha}{360}\pi)$	2
Hybrid-I (b)	0.5	0.5	1	$4\sin^2(\frac{90-\alpha}{360}\pi)$	$4\sin^2(\frac{90-\alpha}{360}\pi)$	2
Hybrid-I (c)	0.5	1.5	1	$4\sin^2\frac{\pi}{8}$	$4\sin^2\frac{\pi}{8}$	2
Hybrid-II	1	1	1	$4\sin^2(\frac{90-\alpha}{360}\pi)$	$4-4\sin^2(\frac{\alpha}{360}\pi)$	$4\sin^2(\frac{\alpha}{360}\pi)$

0 to 90. The projection of signal points on the Y- (X-)coordinate axis takes four values, $-\Delta_1$, $-\Delta_2$, Δ_1, and Δ_2, where

$$\Delta_1 = \sin\left(\frac{90-\alpha}{360}\pi\right)$$
$$\Delta_2 = \cos\left(\frac{90-\alpha}{360}\pi\right) \tag{1}$$

respectively, for unitary radius. Also considered are 16-QAM constellations such as those depicted in Fig. 1(b), with point coordinates in the set $\{\pm\Delta_1, \pm\Delta_2\}$ and normalized to $\Delta_1^2 + \Delta_2^2 = 1$.

III. Error Performance Analysis of Coded Asymetric 8-PSK Modulation with Multistage Decoding and UEP

In this section, upper bounds are derived on the bit-error probability for coded asymmetric 8-PSK modulations and the three types of unconventional partitionings represented in Fig. 2 over the AWGN channel. These upper bounds are union bounds defined from the evaluation of pairwise-error probabilities. The corresponding parameters are given as follows in Table I: hybrid-I: a) $0 < \alpha < 45$; b) $45 < \alpha < 90$; and c) $\alpha = 45$ in which $N_j (j = 1, 2, 3)$ denotes the average number of nearest neighboring signal points at the jth partitioning level and δ_j^2 denotes the intra-set SED. For $j = 1, 2, 3$, let C_j be the binary (n, k_j, d_j) error correcting code applied as a component code to the jth level, and let $A_w^{(j)}$ denote the number of codewords of weight w in C_j.

A. Upper Bounds on BER with Block Partitioning

In block partitioning [2], signal points in a subset are contained in disjoint half planes, as shown in Fig. 2(a). At the first and second partitioning levels, the average number of nearest neighbor sequences is $(1/2)^{d_i} A_{d_i}^{(i)}$ with $i = 1, 2$, respectively, as opposed to $2^{d_i} A_{d_i}^{(i)}$ for Ungerboeck partitioning [9]. This reduction in error coefficient is realized at the expense of a nonincreasing intra-set distance at each level of the partitioning. Consequently, the first decoding stage achieves an impressive coding gain, but the third decoding stage degrades in performance. These characteristics can be refined with an asymmetric constellation by choosing different values of α in Fig. 2(a). Note that, as expected, in the limiting case $\alpha = 0$, the constellation of Fig. 2(a) tends to a Gray mapped quadrature phase-shift keying (QPSK) constellation indexed by the first two label bits.

Decoding and the associated error performance analysis can be given in the same fashion as for the symmetric constellation case [2], and are briefly reviewed in the following. Note that the decision regions in this case cannot be replicated by w orthogonal two-dimensional constellations in contrast with the cases treated in [10], because different code sequences share the same decision regions as can be seen in Fig. 2(a).

Assume the all-zero codeword is transmitted in the first (second) level, and define $\boldsymbol{c}_w \in C_j\,(j = 1, 2)$ as the decoded codeword of Hamming weight w. Decoding can be achieved by using the projection of the received signal components on the X- (Y-)coordinate axis. Consider, for the nonzero positions of $\boldsymbol{c}_w$, i components of the corresponding signal sequence have projection value Δ_1 and the other $(w - i)$ components have projection value Δ_2. The SED between the transmitted signal sequence and the decision hyperplane $X_1 + X_2 + \cdots + X_w = 0$ associated with this pairwise error is given by [2]

$$d_P^2(i) = \frac{1}{w}\left(i\Delta_1 + (w-i)\Delta_2\right)^2 \tag{2}$$

where Δ_1 and Δ_2 vary with the choice of α, as indicated by (1). Note that the number of such hyperplanes is $\binom{w}{i}$ among the total 2^w error events.

Assuming encoding in systematic form, the probability of a bit error P_{b_j} over the AWGN channel, with a nonuniform 8-PSK

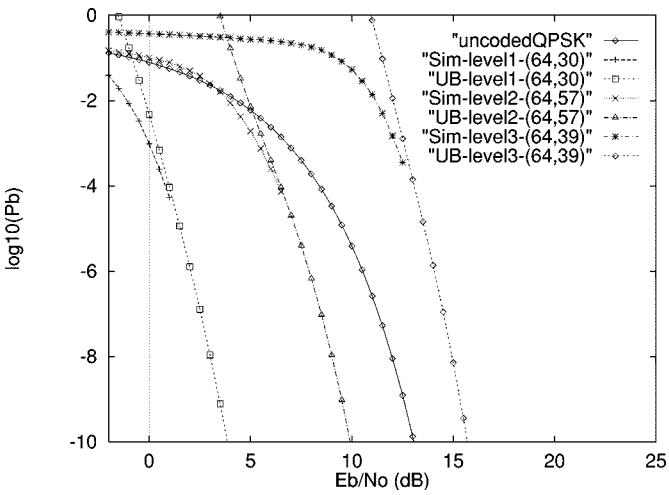

Fig. 3. Upper bounds and simulation results for an asymmetric 8-PSK constellation with $\alpha = 22.5$ and block partitioning.

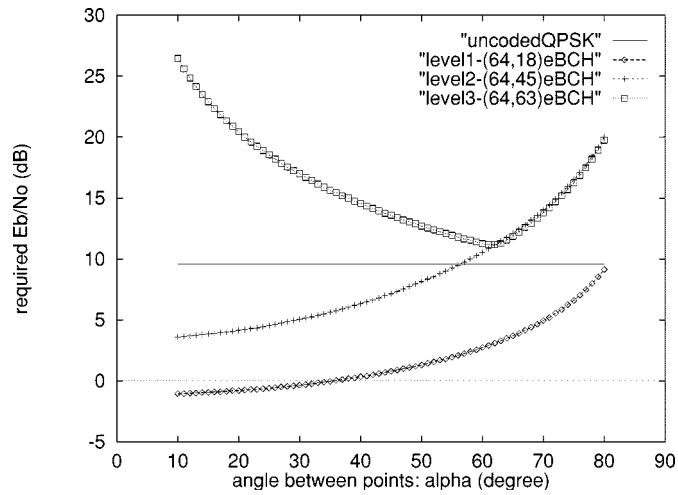

Fig. 4. Required E_b/N_0 at $P_b = 10^{-5}$ with nonuniform 8-PSK and parameter α: block partitioning.

constellation and block partitioning, at level j, $j = 1, 2$, can be upper bounded by union bound arguments as [12]

$$P_{b_j} \le P_{b_j}^{\star} \triangleq \sum_{w=d_j}^{n} \frac{w}{n} A_w^{(j)} 2^{-w} \sum_{i=0}^{w} \binom{w}{i} Q\left(\sqrt{\frac{2RE_b}{N_0} d_P^2(i)}\right) \quad (3)$$

where $R = (k_1+k_2+k_3)/n$ is the overall rate of the multilevel code in bits/symbol, E_b/N_0 denotes the energy per information bit to noise ratio, and

$$Q(x) = \frac{1}{\sqrt{2\pi}} \int_x^{\infty} e^{-n^2/2}\, dn. \quad (4)$$

An upper bound on bit-error probability for the third level of nonuniform 8-PSK constellations can be obtained by simple union bound arguments, with $\delta_3 = 2\sin((\alpha/360)\pi)$, as

$$P_{b_3} \le P_{b_3}^{\star} \triangleq \sum_{w=d_3}^{n} \frac{w}{n} A_w^{(3)} Q\left(\sqrt{\frac{RE_b}{2N_0} w\delta_3^2}\right). \quad (5)$$

However, these bounds do not consider propagation of errors between stages, which is expected with extreme α values. To encompass error propagation effects to the third decoding stage, the results in [2] are extended to approximate the upper bound as

$$P_{b_3} \le P_{b_3}^{\star} + \frac{1}{2} P_{b_1}^{\star} + \frac{1}{2} P_{b_2}^{\star}. \quad (6)$$

Note that there does not occur any error propagation from the first stage to the second because the corresponding decoding processes are independent.

B. Results for Block Partitioning

The upper bounds derived above are compared with computer simulations in Fig. 3. The component codes are the (64, 30, 14) extended BCH (ex-BCH) code for the first level, the (64, 57, 4) ex-BCH code for the second level, and the (64, 39, 10) ex-BCH code for the third level of block partitioning. The angle in Fig. 1(a) is set to $\alpha = 22.5$, and the overall rate of this multilevel code is $R = 1.968\,75$ bits/symbol. Soft decision decoding based on ordered statistics [13] was applied to all the simulations in this paper, with sufficient reprocessing order to achieve practically optimum performance at each decoder stage. It can be observed that the upper bounds in (3) and (6) are tight, and that this multilevel code shows three levels of error protection capability, with proportions of bits at each level different from those reported in [2].

The required E_b/N_0 to achieve $P_b = 10^{-5}$, where the bound is sufficiently tight, is calculated in Fig. 4 by the upper bounds in (3) and (6) as a function of α for a nonuniform 8-PSK constellation. The component codes are the (64, 18, 22), (64, 45, 8), and (64, 63, 2) ex-BCH codes at the first, second, and third levels, respectively. The overall rate is $1.968\,75$ bits/symbol. The required E_b/N_0 to achieve the same bit-error probability with uncoded QPSK is also shown as a reference. Compared with uniform 8-PSK constellations ($\alpha = 45$), a lower bit-error probability can be provided at the first and second levels in nonuniform 8-PSK constellations if α is smaller than 45, due to the enhanced intra-set distances. On the other hand, the performance of the third level degrades because the signal points within a quadrant get closer for smaller values of α. For this choice of component codes, good tradeoffs in error performance between the three decoding stages are possible for $\alpha < 60$. For $\alpha > 60$, the error performance of the second decoding stage becomes worse than that of the third stage, provided correct decisions at the second stage were made. However, as shown in Fig. 4, errors propagate so that both stages have about the same error performance.

C. Upper Bounds on BER with Hybrid-I Partitioning

Hybrid-I partitioning [2] for 8-PSK constellation is realized by introducing Ungerboeck partitioning at the second level, as shown in Fig. 2(b). Therefore, the error performance of the first level is the same as for block partitioning. On the other hand, the intra-set distance of the third partitioning level is enhanced to $\delta_3^2 = 2$ regardless of α, with increased average nearest signal sequences at the second level, as discussed later. By proper choice of the component codes, the error performances of the last two

levels can be balanced out so that two levels of error protection are achieved.

For $\alpha < 45$, the average number of nearest signal points in Fig. 2(b) is one at the second partitioning level. However, for half the points in each half-plane corresponding to the decoding of first stage, a second neighbor (at greater distance) exists, which results in increased multiplicity, as shown in the following. On the other hand, for $\alpha > 45$, only one of the two points has one nearest signal point, while both have one nonnearest neighbor. Note that symmetric constellation with $\alpha = 45$ is the intersection of these two cases in which all the neighbors have equivalent contributions.

For a nonuniform 8-PSK constellation, the upper bounds on the BER for the first and third levels are the same as for block partitioning, and are given by (3) and (5), respectively, after modifying the value δ_3. Next, a union bound on the error performance of the second stage for hybrid-I partitioning is presented. This bound is derived by evaluating the pairwise-error probability associated with each possible error sequence. Note that the distribution of neighboring signal points differs from that considered in the analysis of uniform 8-PSK given in [2]. For signal points whose projection value on the X-coordinate axis is $\pm\Delta_2$ (referred to as "inner points" in the following), the SED to the two neighboring points are $D_1^2 = 4\sin^2(\alpha\pi/360)$ and $D_2^2 = 4\sin^2((90-\alpha)\pi/360)$, respectively. The other signal points (referred to as "outer points") have one nearest signal point at distance $D_1^2 = 4\sin^2(\alpha\pi/360)$.

In evaluating the pairwise-error probability, again the SED between transmitted and decoded sequence is needed. As opposed to the derivation of (3) a distinct decision region is associated with each pair of code sequences considered. Consequently, Pythagoras' theorem holds. Assume without loss of generality that the all-zero sequence is transmitted at the second level and denote by w the weight of an incorrectly decoded codeword $\boldsymbol{c}_w$ at the second level. As an "inner point" (or "outer point") is selected with probability 1/2, it can be assumed that $i(0 \le i \le w)$ "inner points" (signal points with label "$x00$" in which x is arbitrary) and $(w-i)$ "outer points" ("$x01$") are transmitted. For this codeword $\boldsymbol{c}_w$, consider an error event in which, for the i transmitted "inner points," $j(0 \le j \le i)$ symbols correspond to erroneous "inner points" ("$x11$") at distance D_2^2, and the remaining $(i-j)$ symbols correspond to erroneous "outer points" ("$x10$") located at D_1^2. The $(w-i)$ transmitted "outer points" have only one nearest neighbor located at D_1^2. It follows from Pythagoras' theorem that the SED between the transmitted sequence and the incorrectly decoded codeword can be expressed as

$$\begin{aligned} d_P^2 &= (i-j)D_1^2 + jD_2^2 + (w-i)D_1^2 \\ &= (w-j)D_1^2 + jD_2^2. \end{aligned} \tag{7}$$

From union bound arguments, an upper bound on the error performance with respect to the second decoding stage is given by

$$\begin{aligned} P_{b_2} &\le P_{b_2}^{\star} \\ &\triangleq \sum_{w=d_2}^{n} \frac{w}{n} A_w^{(2)} 2^{-w} \sum_{i=0}^{w} \sum_{j=0}^{i} \binom{w}{i}\binom{i}{j} Q\left(\sqrt{\frac{RE_b}{2N_0} d_P^2}\right). \end{aligned} \tag{8}$$

With error propagation, the upper bounds can be again approximated by

$$\begin{aligned} P_{b_1} &\le P_{b_1}^{\star} \\ P_{b_2} &\le P_{b_2}^{\star} + \frac{1}{2} P_{b_1} \\ P_{b_3} &\le P_{b_3}^{\star} + \frac{1}{2} P_{b_2}. \end{aligned} \tag{9}$$

It should be noted that (9) can give an overestimation of error propagation from the second to the third decoding stages. This is true especially when α is small, because the labeling of the third partitioning level can be viewed as block partitioning. In this case, however, a better code design can be found and the issue of error propagation is not investigated further.

D. Approximated Bound for the Second Stage of Hybrid-I Partitioning

In the following, a simple approximation of (8) based on Pythagoras' theorem with respect to the constellations of Fig. 2(b) is derived. Consider first the case $\alpha < 45$. As mentioned previously, "inner points" have two neighboring signal points at the SED D_1^2 and D_2^2, respectively. This implies that the two corresponding decision boundaries DL_1 and DL_2 are located at the SED $D_1^2/4$ and $D_2^2/4$, respectively. Let us consider how much effects these neighboring signal points totally have when that of the closest signal point is normalized to 1. This defines *effective number of nearest neighbors*, extending the conventional concepts in [2], [14], and [15] where the number of neighboring signal points is counted only for symmetric constellations. For a transmitted signal point $\boldsymbol{s}$ and the corresponding received signal point $\boldsymbol{r}$, define the likelihood ratio L_α as

$$\begin{aligned} L_\alpha &= \frac{p(|\boldsymbol{r}-\boldsymbol{s}|^2 = D_2^2/4|\boldsymbol{s})}{p(|\boldsymbol{r}-\boldsymbol{s}|^2 = D_1^2/4|\boldsymbol{s})} \\ &= \frac{\exp\left(-\frac{RE_b}{N_0}\frac{D_2^2}{4}\right)}{\exp\left(-\frac{RE_b}{N_0}\frac{D_1^2}{4}\right)} \\ &= \exp\left\{-\frac{RE_b}{4N_0}(D_2^2 - D_1^2)\right\}. \end{aligned} \tag{10}$$

This definition suggests that the *effective number of nearest neighbors* associated with "inner points" can be estimated as $(1+L_\alpha)$ with respect to the SED D_1^2. Note that hybrid-I partitioning with symmetric 8-PSK modulation ($\alpha = 45$) is a special case with $L_\alpha = 1$. Since half of the points ("inner points") in Fig. 2(b) correspond to this case, and half of the points ("outer points") have only one nearest neighbor, the *effective error coefficient* B_w associated with the SED wD_1^2 for hybrid-I partitioning becomes

$$\begin{aligned} B_w &= \sum_{i=0}^{w} 2^{-w} A_w^{(2)} \binom{w}{i} 1^{w-i} (1+L_\alpha)^i \\ &= (1+L_\alpha/2)^w A_w^{(2)}. \end{aligned} \tag{11}$$

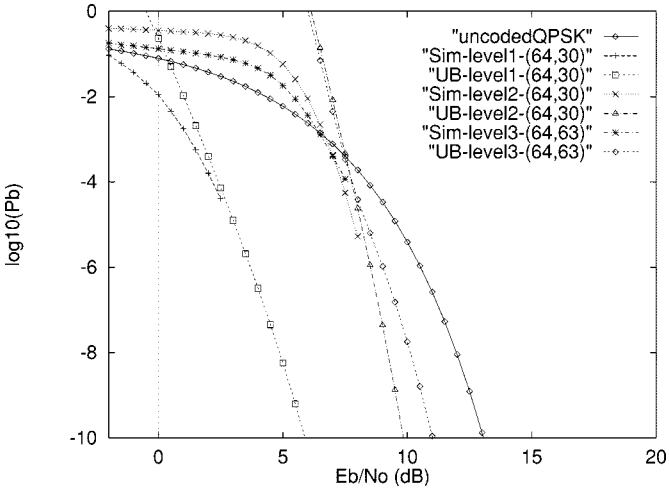

Fig. 5. Upper bounds and simulation results for an asymmetric 8-PSK constellation with $\alpha = 40$ and hybrid-I partitioning.

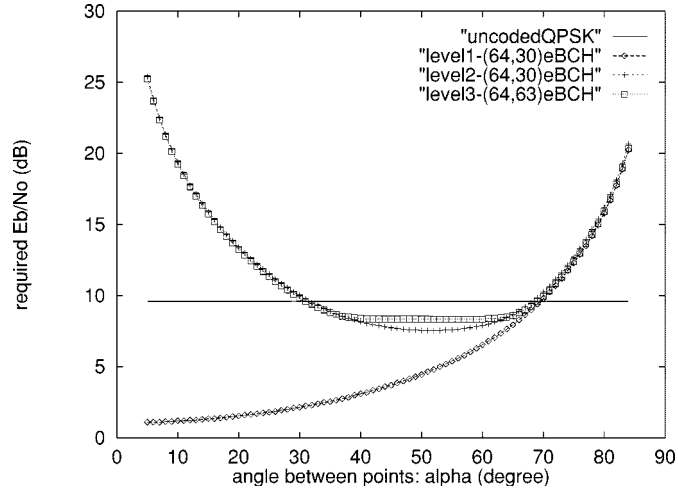

Fig. 6. Required E_b/N_0 at $P_b = 10^{-5}$ with nonuniform 8-PSK constellations and parameter α: hybrid-I partitioning.

The same arguments as in [2] can now be applied to obtain an approximation for an upper bound on the error performance of the second level, which results in

$$P_{b_2} \le P_{b_2}^{\star} \triangleq \sum_{w=d_2}^{n} \frac{w}{n} B_w Q\left(\sqrt{\frac{RE_b}{2N_0} w D_1^2}\right). \qquad (12)$$

If α is larger than 45, then $D_1 \ge D_2$ and the effective number of nearest neighbors for an "inner point" becomes $(1 + 1/L_\alpha)$, and $1/L_\alpha$ for "outer points." Therefore, for $\alpha > 45$, the *effective error coefficient* is defined as

$$\begin{aligned} B_w &= \sum_{i=0}^{w} 2^{-w} A_w^{(2)} \binom{w}{i} (1/L_\alpha)^{w-i} (1 + 1/L_\alpha)^i \\ &= (1/2 + 1/L_\alpha)^w A_w^{(2)} \end{aligned} \qquad (13)$$

and $P_{b_2}^{\star}$ is defined as in (12) after replacing D_1^2 by D_2^2.

In [15] and [16], it is pointed out that for uniform constellations and multistage decoding, the effective error coefficient can be expressed as the product of: 1) the number of component codewords with Hamming weight w and 2) the wth power of the average number of nearest signal points for each signal point in a subset, for QAM constellations with Ungerboeck-type partitioning. The above technique can be regarded as a generalization to asymmetric constellations, to consider the effects of second nearest neighbor points, when Pythagoras' theorem applies.

E. Results for Hybrid-I Partitioning

As an example, component codes are selected as the (64, 30, 14) ex-BCH code both at the first and second levels, and the (64, 63, 2) ex-BCH code at the third level. The angle is set to $\alpha = 40$ and the overall code rate is $R = 1.921\,875$ bits/symbol. The curves derived from (8) and (12) overlap at all signal-to-noise ratio (SNR) values, as expected. The simulation results and corresponding union bounds, for all levels are depicted in Fig. 5 together with the performance of uncoded QPSK. Two levels of UEP are provided with relatively small proportion of MIB.

Due to the tightness of the upper bounds at the BER 10^{-5}, these bounds can be used to devise a UEP coded system as for block partitioning. In Fig. 6, the required E_b/N_0 to achieve $P_b = 10^{-5}$ is calculated based on the derived bounds for the hybrid-I partitioning and uncoded QPSK. The component codes are the (64, 30, 14), (64, 30, 14), and (64, 63, 2) ex-BCH codes at the first, second, and third levels, respectively, and the overall code rate is $R = 1.921\,875$ bits/symbol. For $\alpha < 40$, the multilevel code has two levels of protection, while for $40 < \alpha < 60$, error propagation from second to third decoding stage is not as severe. The required E_b/N_0 for the third level is constant within this range, because the intra-set distance of the third partitioning level is constant regardless of α. If α becomes too large, then the error performance of the first level dominates the other levels and errors propagate.

F. Upper Bounds on BER with Hybrid-II Partitioning

Another partitioning scheme in Fig. 2(c), referred to as hybrid-II [8], is given by clustering signal points and labeling according to Ungerboeck set partitioning rules at lower index levels. Compared with block partitioning, the intra-set distance at the second level is enhanced at the cost of increasing the number of decision regions for the first level. In the limiting case $\alpha = 0$, this partitioning naturally becomes an Ungerboeck mapped QPSK constellation.

With hybrid-II partitioning, upper bounds on the bit-error probability for the second- and third-stage decoders follow directly from the union bound,

$$P_{b_j} \le P_{b_j}^{\star} \triangleq \sum_{w=d_j}^{n} \frac{w}{n} A_w^{(j)} Q\left(\sqrt{\frac{RE_b}{2N_0} w \delta_j^2}\right), \qquad j = 2, 3. \qquad (14)$$

However, at the first decoding stage, the effect of nonnearest neighbors cannot be ignored when α decreases and Pythagoras' theorem no longer holds since different pairs of code sequences share the same decision region in Fig. 2(c). In this case, the union bound should be considered in terms of the cluster containing two signal points of a quadrant. Due to the symmetry of the decision regions in Fig. 2(c) with respect to the first-stage

labeling, it can be assumed that the all-zero sequence is transmitted at all the levels without loss of any generality due to the uniform symmetry of the constellation. That is, all the transmitted signals are labeled "000." As before, define w as the Hamming weight of an erroneous decoded codeword $\boldsymbol{c}_w$ at the first stage. By considering the w-dimensional decision hyperplane corresponding to $i(0 \le i \le w)$ X-coordinate axes and $(w-i)$ Y-coordinate axes with respect to Fig. 2(c), the associated pairwise-error probability can be derived based on the SED between the transmitted signal sequence representing the all-zero codeword and this hyperplane, which can be expressed in the same form as (2). As a result, a union bound for the first decoding stage of hybrid-II partitioning is given by

$$P_{b_1} \le P_{b_1}^{\star} \triangleq \sum_{w=d_1}^{n} \frac{w}{n} A_w^{(1)} \sum_{i=0}^{w} \binom{w}{i} Q\left(\sqrt{\frac{2RE_b}{N_0}\, d_P^2(i)}\right) \tag{15}$$

where $d_P^2(i)$ is given in (2). Again, (9) based on (14) and (15) is used to include error propagation.

G. Approximated Bound for the First Stage of Hybrid-II Partitioning

The upper bound (15) for the first decoding stage becomes loose when a powerful component code (with large minimum Hamming distance) and small values of α are chosen, due to the important overlappings of decision regions in the $2w$-dimensional space associated with $\boldsymbol{c}_w$.

Based on Fig. 2(c), a similar approximation as for hybrid-I partitioning follows after defining:

$$L_\alpha = \frac{\exp\left(-\frac{RE_b}{N_0}\Delta_2^2\right)}{\exp\left(-\frac{RE_b}{N_0}\Delta_1^2\right)} = \exp\left\{-\frac{RE_b}{N_0}(\Delta_2^2 - \Delta_1^2)\right\}. \tag{16}$$

Note that all the signal points have now the same distribution of neighbors. An approximated upper bound for the error performance of the first level of hybrid-II partitioning is obtained by regarding $(1+L_\alpha)$ as the *effective number of nearest neighbors* associated with any signal point in Fig. 2(c), so that

$$P_{b_1} \le P_{b_1}^{\star} \triangleq \sum_{w=d_1}^{n} \frac{w}{n} A_w^{(1)} (1+L_\alpha)^w Q\left(\sqrt{\frac{RE_b}{2N_0} w \delta_1^2}\right). \tag{17}$$

Equation (17) follows from applying Pythagoras' theorem from Fig. 2(c) to the $2w$-dimensional space associated with the error event of weight w considered. Although not exact since (15) cannot be derived based on Pythagoras' theorem [as opposed to (7)], this approach provides a simple yet tight approximation which can be justified by simple geometrical arguments.

H. Results for Hybrid-II Partitioning

As an example, consider as component codes the (64, 30, 14) ex-BCH code at the first level, the (64, 57, 4) ex-BCH code at the second level, and the (64, 39, 10) ex-BCH code at the third level. The angle is set to $\alpha = 30$, and the overall rate of this multilevel code is $R = 1.96875$ bits/symbol.

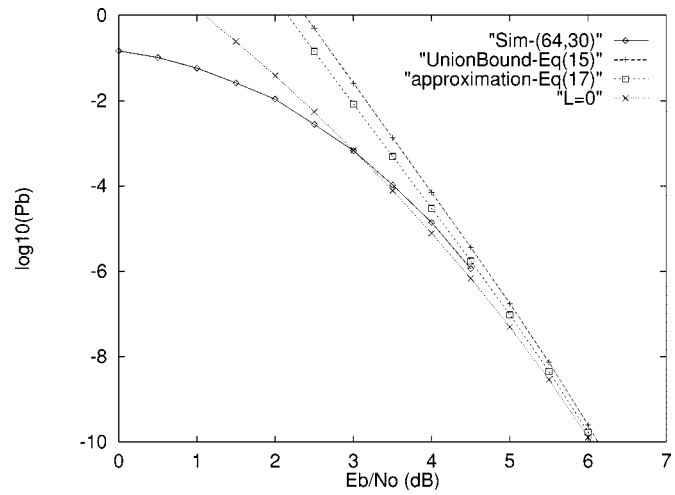

Fig. 7. Upper bounds and simulation results for first-stage decoding: asymmetric 8-PSK constellation with $\alpha = 30$ and hybrid-II partitioning.

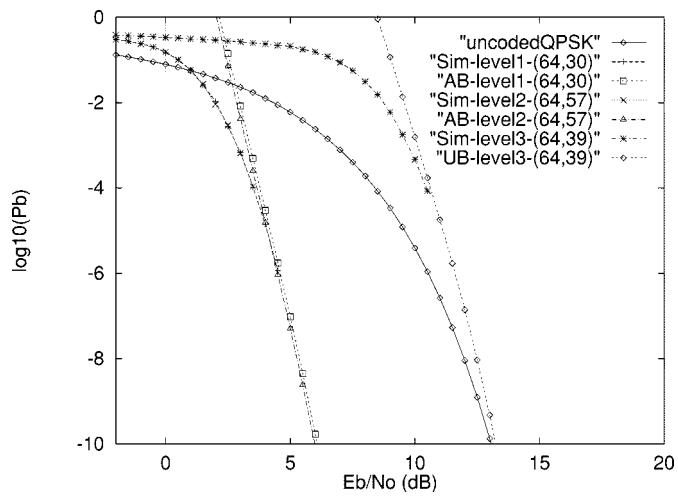

Fig. 8. Upper bounds and simulation results for an asymmetric 8-PSK constellation with $\alpha = 30$ and hybrid-II partitioning (AB: approximated bound).

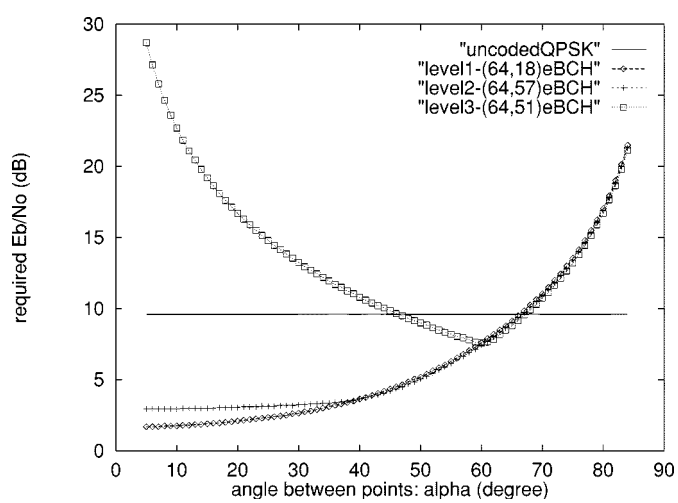

Fig. 9. Required E_b/N_0 at $P_b = 10^{-5}$ with nonuniform 8-PSK and parameter α: hybrid-II partitioning.

In Fig. 7, simulation results of the first level are compared with (15) and (17). As a reference, the truncated union bound

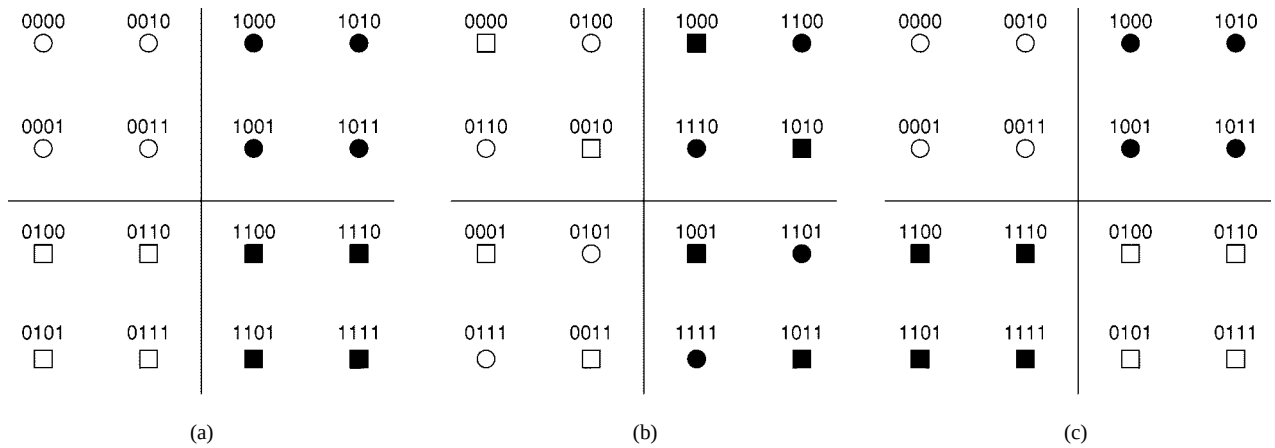

Fig. 10. Signal labeling of 16-QAM constellation with: (a) block partitioning; (b) hybrid-I partitioning; and (c) hybrid-II partitioning.

TABLE II
PARAMETERS ASSOCIATED WITH PARTITIONINGS OF A 16-QAM ASYMMETRIC CONSTELLATION

Partitioning	N_1	N_2	N_3	N_4	δ_1^2	δ_2^2	δ_3^2	δ_4^2
Block	0.5	0.5	1	1	$4\Delta_1^2$	$4\Delta_1^2$	$(\Delta_2-\Delta_1)^2$	$(\Delta_2-\Delta_1)^2$
Hybrid-I (a)	0.5	0.5	0.5	1	$4\Delta_1^2$	$4\Delta_1^2$	$(\Delta_2-\Delta_1)^2+4\Delta_1^2$	$(\Delta_2+\Delta_1)^2$
Hybrid-I (b)	0.5	2	1	1	$4\Delta_1^2$	$(\Delta_2-\Delta_1)^2$	$2(\Delta_2-\Delta_1)^2$	$(\Delta_2+\Delta_1)^2$
Hybrid-I (c)	0.5	2.5	1.5	1	0.4	0.4	0.8	1.6
Hybrid-II	1	0.25	1	1	$4\Delta_1^2$	$8\Delta_1^2$	$(\Delta_2-\Delta_1)^2$	$(\Delta_2-\Delta_1)^2$

assuming only one nearest signal point ("$L = 0$" in Fig. 7) is also plotted. The approximation in (17) meets the simulation results for BER's lower than 10^{-5} and is tighter than the exact union bound. In addition, it can be observed that considering only the nearest signal point ($L_\alpha = 0$) does not give an upper bound for this value of α. Simulation results and union bounds for all levels are included in Fig. 8 and compared with uncoded QPSK.

In Fig. 9, the required E_b/N_0 to achieve $P_b = 10^{-5}$ is depicted for the hybrid-II partitioning and uncoded QPSK. The component codes are the (64, 18, 22), (64, 57, 4), and (64, 51, 6) ex-BCH codes at the first, second, and third levels, respectively. The overall code rate is $1.968\,75$ bits/symbol. Three protection levels are possible for $\alpha < 35$, and only two for $35 < \alpha < 60$.

IV. ERROR PERFORMANCE ANALYSIS OF CODED ASYMETRIC 16-QAM MODULATION WITH MULTISTAGE DECODING AND UEP

In this section, multilevel UEP coded modulation based on asymmetric 16-QAM is analyzed for the AWGN channel. This is because compared with asymmetric PSK signaling, in some cases new considerations are necessary when evaluating the corresponding error performances. 16-QAM constellations with block, hybrid-I, and hybrid-II partitioning are depicted in Fig. 10(a)–(c), respectively. The parameters associated with the three partitionings are compared in Table II (hybrid-I: a) $0 < \Delta_1 < 1/\sqrt{10}$; b) $1/\sqrt{10} < \Delta_1 < 1/\sqrt{2}$; and c) $\Delta_1 = 1/\sqrt{10}$) where $N_j (j = 1, 2, 3, 4)$ denotes the average number of nearest neighboring signal points at jth partitioning level.

For $j = 1, 2, 3, 4$, let C_j be the linear binary (n, k_j, d_j) error correcting code applied as component code to jth level, and let $A_w^{(j)}$ denote the number of codewords of weight w in C_j. Let $R = (k_1 + k_2 + k_3 + k_4)/n$ bits/symbol be the rate of the multilevel code.

A. Upper Bounds on BER and Results with Block Partitioning

The derivation of the upper bound on the BER for block partitioning with the 16-QAM constellation depicted in Fig. 10(a) follows the same line of arguments as for 8-PSK constellations. The bound for the first and second levels can be represented by (3) after replacing Δ_1 and Δ_2 in (2) by proper values. Based on the union bound, upper bounds on the bit-error probability for the third and fourth decoding stages of the 16-QAM constellations considered are given by

$$P_{b_j} \le P_{b_j}^\star \triangleq \sum_{w=d_j}^{n} \frac{w}{n} A_w^{(j)} Q\left(\sqrt{\frac{RE_b}{2N_0} w(\Delta_2-\Delta_1)^2}\right), \quad j = 3, 4. \tag{18}$$

The required E_b/N_0 to achieve $P_b = 10^{-5}$, where the bound is sufficiently tight, is depicted in Fig. 11 as a function of Δ_1 for nonuniform 16-QAM constellations. The component codes are the (64, 18, 22) ex-BCH, (64, 24, 16) ex-BCH, (64, 36, 12) ex-BCH, and (64, 45, 8) ex-BCH codes. The overall rate is $1.921\,875$ bits/symbol. The same behavior as for 8-PSK with block partitioning is observed. That is, for the first and second levels, the error performance is enhanced with larger values of Δ_1 due to the increased intra-set distance, at the expense of larger bit-error probabilities for the remaining levels.

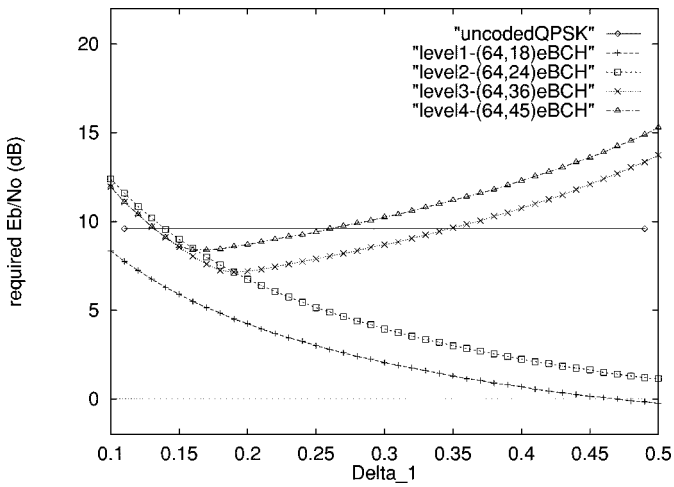

Fig. 11. Required E_b/N_0 at $P_b = 10^{-5}$ with nonuniform 16-QAM and parameter Δ_1: block partitioning.

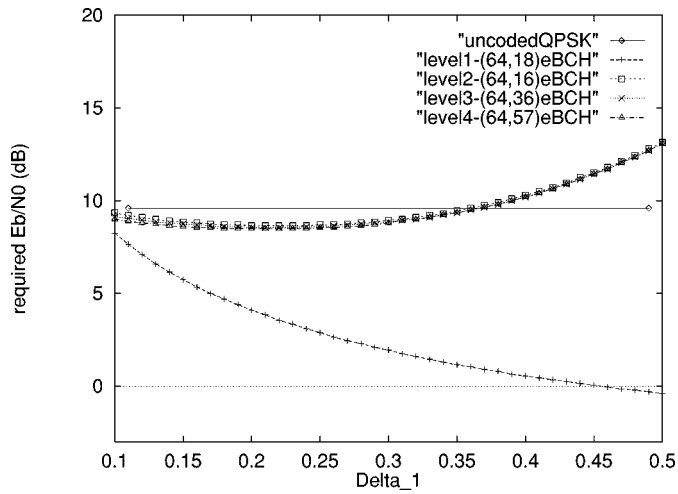

Fig. 12. Required E_b/N_0 at $P_b = 10^{-5}$ with nonuniform 16-QAM and parameter Δ_1: hybrid-I partitioning.

B. Results of Hybrid-I Partitioning

Hybrid-I partitioning [2], originally proposed for uniform 8-PSK and 64-QAM, can be extended to asymmetric 16-QAM constellations as shown in Figs. 10(b) and 1(b). The first partitioning level is realized with block partitioning while the other partitionings are done with Ungerboeck partitioning.

The theoretical analysis of this scheme follows the same lines as [2] and Section III. The required E_b/N_0 at $P_b = 10^{-5}$ is calculated as a function of Δ_1 in Fig. 12. The component codes selected are the (64, 18, 22), (64, 16, 24), (64, 36, 12), and (64, 57, 4) ex-BCH codes, with an overall code rate $R = 1.984\,375$. In this case, two levels of error correcting capability are obtained with a relatively small proportion of MIB well protected for Δ_1 large enough. Note that the derived bounds at levels 2–4 are not very tight, because of the large multiplicity at the second level and the associated error propagation to third and fourth decoding stages. Consequently, the actual required E_b/N_0 is about 0.5 dB better than that plotted in the figure.

C. Upper Bounds on BER with Hybrid-II Partitioning

While both block and hybrid-I partitionings with QAM signaling follow the same analyses as those derived in Section III for PSK signaling, new considerations have to be brought to hybrid-II partitioning for QAM signaling. Compared with block partitioning (see Table II), hybrid-II partitioning has a larger average error coefficient at the first level (1 versus 0.5), but has both a smaller average error coefficient and a larger intra-set distance at the second level. This implies that a weaker code can be used at the second level of the hybrid-II partitioning, and therefore allows to assign more information bits. As a result, hybrid-II partitioning achieves larger proportion of MIB at the cost of a degradation in error performance.

1) First Decoding Stage: Again, and without loss of generality, assume that the all-zero codeword is transmitted at the first level, and due to the symmetry of the labeled constellation with respect to the second level, consider that the all-zero codeword is also transmitted at the second level. Recall that for multistage decoding, any n-tuple is a valid candidate codeword at the remaining levels. Let w denote the Hamming weight of a decoded codeword $\boldsymbol{c}_w \in C_1$. Then, at the first-stage decoder, $\mathbf{c}_w$ defines $2w$-dimensional decision hyperplanes again consisting of either X- or Y-coordinate axes from w two-dimensional spaces.

Assume that among the corresponding w symbols, $i(0 \le i \le w)$ symbols are transmitted as "0011," $j(0 \le j \le (w-i))$ symbols are transmitted as "0000," and $(w-i-j)$ symbols as "0010" or "0001." Note that there exist 2^{w-i-j} possibilities of signal point selections among "0010" and "0001." Due to the symmetry of the points "0010" and "0001" with respect to the X- and Y-coordinate axes, assume first, without loss of generality, that all the $(w-i-j)$ signal points are transmitted as "0010." The corresponding symbols are associated with $(w-i-j)$ dimensions obtained from a combination of X- and Y-coordinate axes. Consider the w-dimensional hyperplane formed from $k(0 \le k \le (w-i-j))$ Y-coordinate axes and $(w-i-j-k)$ X-coordinate axes with respect to "0010." Then the SED between the transmitted signal sequence and this $2w$-dimensional hyperplane can be written as [2]

$$\begin{aligned} d_{P1}^2(w,i,k) &= \frac{1}{w}\left\{i\Delta_1 + j\Delta_2 + k\Delta_1 + (w-i-j-k)\,\Delta_2\right\}^2 \\ &= \frac{1}{w}\left\{(i+k)\Delta_1 + (w-i-k)\Delta_2\right\}^2. \end{aligned} \tag{19}$$

At the first-stage decoder, we have 2^{w-i-j} possibilities of choosing $(w-i-j)$ values among "0001" and "0010," each defining a distinct hyperplane. Also, since both "0000" and "0011" have two nearest neighboring decision regions [see Fig. 10(c)], we have 2^{i+j} corresponding distinct hyperplanes associated with these two labels. Considering all the combinations of variables i, j, and k which define 4^w error events, the corresponding union bound provides the following upper bound on the BER associated with the first decoding stage:

$$P_{b_1} \le P_{b_1}^{\star} \triangleq \sum_{w=d_1}^{n} \frac{w}{n} A_w^{(1)} p_{1w} \tag{20}$$

where

$$\begin{aligned} p_{1w} &= 4^{-w} \sum_{i=0}^{w} \sum_{j=0}^{w-i} \binom{w}{i} \binom{w-i}{j} 2^{i+j} \sum_{k=0}^{w-i-j} 2^{w-i-j} \\ &\quad \cdot \binom{w-i-j}{k} Q\left(\sqrt{\frac{2RE_b}{N_0} d_{P1}^2(w, i, k)}\right) \\ &= 2^{-w} \sum_{i=0}^{w} \sum_{j=0}^{w-i} \sum_{k=0}^{w-i-j} \binom{w}{i} \binom{w-i}{j} \\ &\quad \cdot \binom{w-i-j}{k} Q\left(\sqrt{\frac{2RE_b}{N_0} d_{P1}^2(w, i, k)}\right). \end{aligned} \tag{21}$$

2) Second Decoding Stage: A similar approach provides an upper bound on P_{b_2}, the bit-error probability associated with the second decoding stage. After observing that signal points labeled by "01xx" can be at three possible distances from the decision line $Y = X$ in Fig. 10(c) (namely $D_1 = \sqrt{2}\Delta_1$, $D_2 = \sqrt{2}(\Delta_1 + \Delta_2)/2$, and $D_3 = \sqrt{2}\Delta_2$), the union bound provides

$$P_{b_2} \le P_{b_2}^{\star} \triangleq \sum_{w=d_2}^{n} \frac{w}{n} A_w^{(2)} p_{2w} \tag{22}$$

where

$$\begin{aligned} p_{2w} &= 4^{-w} \sum_{i=0}^{w} \sum_{j=0}^{w-i} \sum_{k=0}^{w-i-j} \binom{w}{i} \binom{w-i}{j} \\ &\quad \cdot \binom{w-i-j}{k} Q\left(\sqrt{\frac{2RE_b}{N_0} d_{P2}^2(w, i, j, k)}\right) \end{aligned} \tag{23}$$

and

$$\begin{aligned} d_{P2}^2(w, i, j, k) &= \frac{1}{w}\{iD_1 + (j+k)D_2 \\ &\quad + (w-i-j-k)D_3\}^2. \end{aligned} \tag{24}$$

3) Third and Fourth Decoding Stages: The bit-error probability for the third and fourth decoding stages of the 16-QAM constellations with hybrid-II partitioning are the same as that of block partitioning given by (18). Finally, (9) is readily extended to the four-stage decoding case to include error propagation.

D. Approximation Techniques for the First Stage of Hybrid-II Partitioning

With the arguments of Section III-G based on Pythagoras' theorem, (21) can be approximated by

$$\begin{aligned} p_{1w} &\approx 2^{-w} \sum_{i=0}^{w} \sum_{j=0}^{w-i} \binom{w}{i} \binom{w-i}{j} \\ &\quad \cdot (1 + L_\alpha)^{w-i-j} Q\left(\sqrt{\frac{2RE_b}{N_0} d_{Pap}^2(w, j)}\right) \end{aligned} \tag{25}$$

where

$$d_{Pap}^2(w, j) = (w-j)\Delta_1^2 + j\Delta_2^2 \tag{26}$$

and

$$L_\alpha = \exp\{-RE_b/N_0(\Delta_2^2 - \Delta_1^2)\}. \tag{27}$$

The value $(1 + L_\alpha)$ can be viewed as the average number of nearest neighbors with respect to the SED Δ_1^2 in the underlying constellation of Fig. 10(c). Hence (25) follows by applying Pythagoras' theorem from Fig. 10(c) to the $2w$-dimensional space associated with the error event of weight w considered. Although not exact, this approach provides a simple and tight approximation as for PSK constellations. This bound is referred to as the *approximated bound* in the following.

Equations (21) and (25) generally provide loose upper bounds even at moderate SNR if the minimum Hamming distance d_1 of the first level component code is relatively large. This is due to the fact that the overlappings of the decision regions considered previously not only are nonnegligible, but also correspond to correct decisions, as suggested from Fig. 10(c). Define $q_l (l = 1, 2)$ as

$$q_l = Q\left(\sqrt{\frac{2RE_b}{N_0}\Delta_l^2}\right), \qquad l = 1, 2. \tag{28}$$

Given that the signal point "0011" is transmitted, the probability of making an error in the two-dimensional space becomes $2q_1(1 - q_1)$. Note that, in the argument of (21), the nearest neighbor is counted as two by ignoring the overlap of erroneous decision regions, and thus the probability of error in two-dimensional space is $2q_1$. Since q_1 corresponds to error events at distance Δ_1 in the two-dimensional space, the effective number of nearest neighbors can be viewed as $2(1 - q_1)$ in this case. Considering i such signal points, the corresponding effective error coefficient can be expressed as $\{2(1 - q_1)\}^i$. The same arguments apply to the signal point "0000," although the contribution to the bound is much smaller. As a result, (25) can be replaced by the following equation

$$\begin{aligned} p_{1w} &\approx 2^{-w} \sum_{i=0}^{w} \sum_{j=0}^{w-i} \binom{w}{i} \binom{w-i}{j} (1-q_1)^i (1-q_2)^j \\ &\quad \cdot (1 + L_\alpha)^{w-i-j} Q\left(\sqrt{\frac{2RE_b}{N_0} d_{Pap}^2(w, j)}\right) \end{aligned} \tag{29}$$

in (20). This bound gives a tighter approximated bound, especially at low SNR, and is called *improved approximated bound* in the following.

E. Results for Hybrid-II Partitioning

The bounds derived in the previous section are compared with simulation results, and subsequently, the performance of the proposed partitioning is discussed based on the bounds.

Consider a coded asymmetric 16-QAM constellation and, as component codes, the (64, 10, 28) ex-BCH code for the first level, the (64, 45, 8) ex-BCH code for second level, the (64, 36, 12) ex-BCH code for third level, and the (64, 36, 12) ex-BCH code for fourth level. The overall rate of this multilevel code is $R = 1.984\,375$ bits/symbol.

In Fig. 13, simulation results of the first-stage decoder are compared with (20) based on (21), (25), and (29), respectively. It is observed that, whereas the first two bounds are loose (about 2 dB away at $P_b = 10^{-5}$), the improved approximated bound is quite tight. Simulation results for all the levels are depicted in

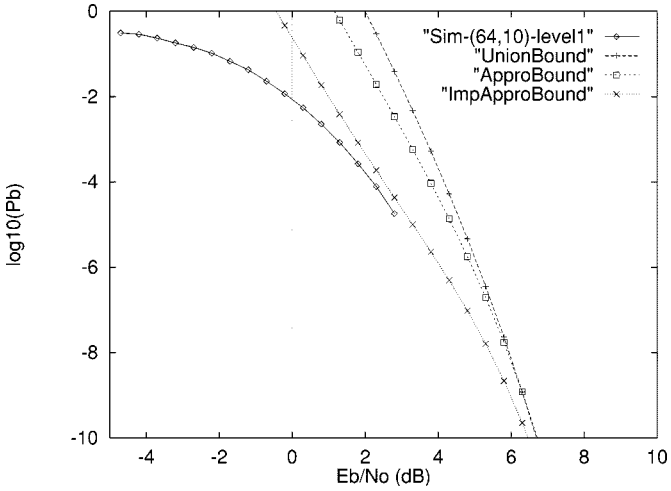

Fig. 13. Upper bounds and simulation results for first-stage decoding: symmetric 16-QAM constellation and hybrid-II partitioning.

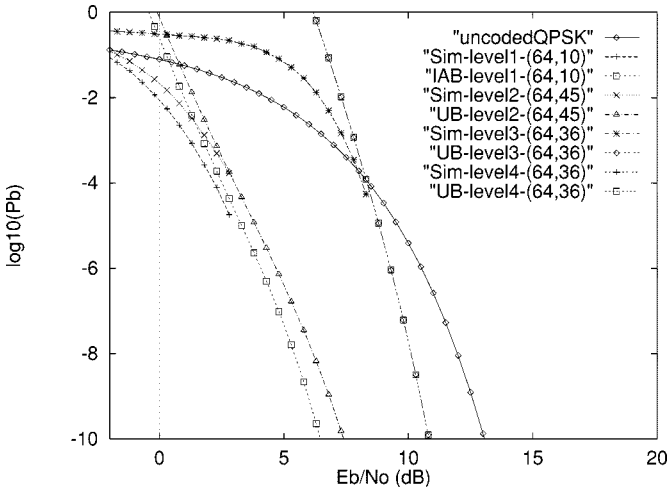

Fig. 14. Upper bounds and simulation results for a symmetric 16-QAM constellation and hybrid-II partitioning (IAB: improved approximated bound).

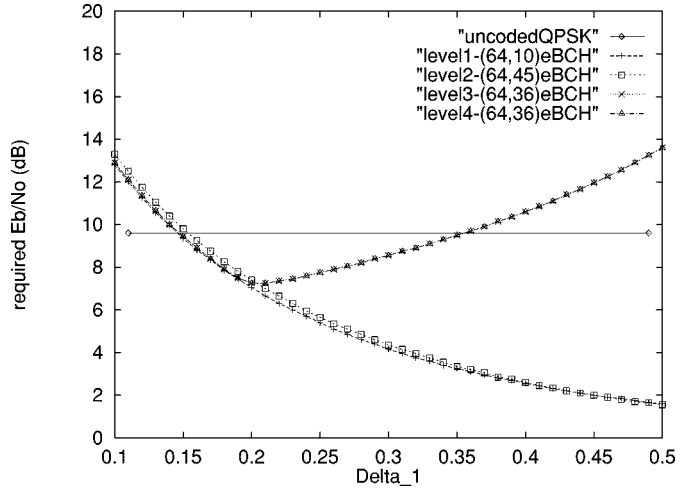

Fig. 15. Required E_b/N_0 at $P_b = 10^{-5}$ with nonuniform 16-QAM and parameter Δ_1: hybrid-II partitioning.

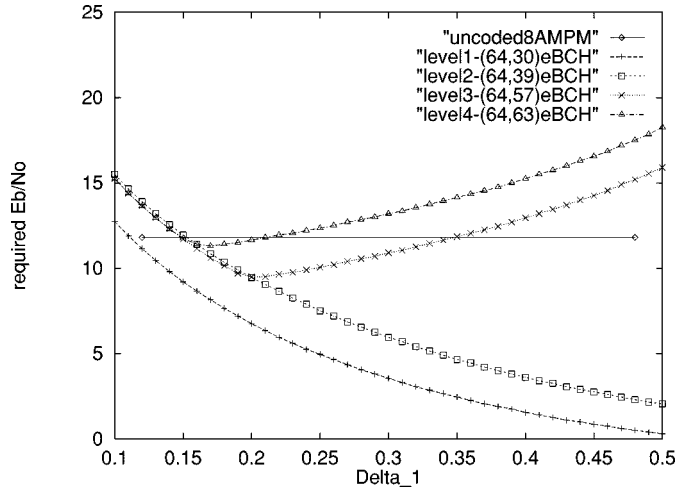

Fig. 16. Required E_b/N_0 at $P_b = 10^{-5}$ with nonuniform 16-QAM and parameter Δ_1: block partitioning (2.953 125 bits/symbol).

Fig. 14 and compared with the best bounds or approximations derived in Sections IV-C and IV-D.

In Fig. 15, the required E_b/N_0 to achieve $P_b = 10^{-5}$, where bounds are sufficiently tight, is calculated as a function of Δ_1. The component codes are the same as above. For small Δ_1, all the four levels show virtually the same performance because of the error propagation from the first (and second) level(s). On the other hand, it can be observed that the first and second levels require smaller E_b/N_0 at a constant BER, as Δ_1 gets larger, while the performance of the third and fourth levels deteriorate.

Finally, it should be noted that the 16-QAM coded modulation schemes with approximately 2 bits/symbol discussed in this section are only for illustration of the tightness of the bounds introduced. That is, this does not preclude the use of a 16-QAM coded modulation scheme with UEP and 3 bits/symbol. In order to increase bandwidth efficiency, it is clear that component codes of larger rates need to be selected, compared to the above cases. This naturally results in relatively weaker error protection capabilities for a given signal constellation. However, this problem can be overcome by again considering asymmetry in the signal constellations. As an example, the required E_b/N_0 at $P_b = 10^{-5}$ has been depicted in Fig. 16 for block partitioning, with a reference of uncoded 8-AMPM constellation. The component codes are (64, 30, 14) ex-BCH code, (64, 39, 10) ex-BCH code, (64, 57, 4) ex-BCH code, and (64, 63, 2) ex-BCH code, respectively, and the overall rate is 2.953 125 bits/symbol. Even with higher rate codes, powerful UEP capabilities can be maintained by choosing proper constellation parameters. This observation further supports the advantages of the multilevel coding with asymmetric modulation and multistage decoding.

V. Conclusion

Multilevel coded modulation with multistage decoding and UEP capabilities have been discussed and analyzed, in conjunction with asymmetry in the signal constellations, to provide more flexibility to the coding scheme. Three types of partitionings have been considered. To illustrate the design guidelines, a theoretical analysis on the bit-error probabilities for 8-PSK and 16-QAM signaling over the AWGN channel has been presented. Upper bounds by union bound arguments

have been derived for each partitioning strategy. The upper bounds are very tight for block partitioning, but become loose in some cases for other hybrid-type partitionings, mainly due to important overlappings of decision regions. To overcome this problem, a tighter simple approximation technique has been proposed. The resulting approximated bounds are tight and, in conjunction with the union bound, can closely predict the performance of multistage decoding of multilevel codes designed from asymmetric constellations. The additional degrees of freedom introduced by the asymmetries provide further refinements which become useful in matching UEP channel coding with hierarchical source coding.

Although this paper focuses on asymmetric 8-PSK and 16-QAM constellations with certain degrees of regularity, the general code constructions and the associated performance analyzes presented can be extended to many more general and arbitrary signaling constellations.

ACKNOWLEDGMENT

The authors would like to thank the anonymous reviewers for their suggestions that were very helpful in improving the quality of the present paper.

REFERENCES

[1] H. Imai and S. Hirakawa, "A new multilevel coding method using error-correcting codes," *IEEE Trans. Inform. Theory*, vol. IT-23, pp. 371–377, May 1977.

[2] R. H. Morelos-Zaragoza, M. P. C. Fossorier, S. Lin, and H. Imai, "Multilevel coded modulation for unequal error protection and multistage decoding—Part I: Symmetric constellations," *IEEE Trans. Commun.*, vol. 48, pp. 204–213, Feb. 2000.

[3] A. R. Calderbank and N. Seshadri, "Multilevel codes for unequal error protection," *IEEE Trans. Inform. Theory*, vol. 39, pp. 1234–1248, July 1993.

[4] L. F. Wei, "Coded modulation with unequal error protection," *IEEE Trans. Commun.*, vol. 41, pp. 1439–1449, Oct. 1993.

[5] G. Taricco and E. Biglieri, "Pragmatic unequal error protection coded schemes for satellite communications," in *Proc. 5th Communication Theory Mini-Conf., GLOBECOM'96*, London, U.K., Nov. 1996, pp. 1–5.

[6] N. Seshadri and C.-E. W. Sundberg, "Multi-level block coded modulation with unequal error protection for the Rayleigh fading channel," *Eur. Trans. Telecommun.*, vol. 4, no. 3, pp. 325–334, May/June 1993.

[7] A. Seeger, "Hierarchical channel coding for Rayleigh and Rice fading," in *Proc. 6th Communication Theory Mini-Conf., GLOBECOM'97*, Phoenix, AZ, Nov. 1997, pp. 208–212.

[8] M. Isaka, R. H. Morelos-Zaragoza, M. P. C. Fossorier, S. Lin, and H. Imai, "Coded modulation for satellite broadcasting based on unconventional partitionings," *IEICE Trans. Fundamentals*, vol. E81-A, no. 10, pp. 2055–2063, Oct. 1998.

[9] G. Ungerboeck, "Channel coding with multilevel/phase signals," *IEEE Trans. Inform. Theory*, vol. IT-28, pp. 55–67, Jan. 1982.

[10] U. Wachsmann, R. F. H. Fischer, and J. B. Huber, "Multilevel codes: Theoretical concepts and practical design rules," *IEEE Trans. Inform. Theory*, vol. 45, pp. 1361–1391, July 1999.

[11] D. Divsalar, M. K. Simon, and J. Yuen, "Trellis coding with asymmetric modulations," *IEEE Trans. Commun.*, vol. COM-35, pp. 130–141, Feb. 1987.

[12] M. P. C. Fossorier, S. Lin, and D. Rhee, "Bit error probability for maximum likelihood decoding of linear block codes and related soft-decision decoding methods," *IEEE Trans. Inform. Theory*, vol. 44, pp. 3083–3090, Nov. 1998.

[13] M. P. C. Fossorier and S. Lin, "Soft-decision decoding of linear block codes based on ordered statistics," *IEEE Trans. Inform. Theory*, vol. 41, pp. 1379–1396, Sept. 1995.

[14] Y. Kofman, E. Zehavi, and S. Shamai (Shitz), "Performance analysis of a multilevel coded modulation system," *IEEE Trans. Commun.*, vol. 42, pp. 299–312, Feb./Mar./Apr. 1994.

[15] T. J. Lunn and A. G. Burr, "Number of neighbors for staged decoding of block coded modulation," *Electron. Lett.*, vol. 29, pp. 1830–1831, Oct. 1993.

[16] G. J. Pottie and D. P. Taylor, "Multilevel codes based on partitioning," *IEEE Trans. Inform. Theory*, vol. 35, pp. 87–98, Jan. 1989.

Motohiko Isaka (S'94–M'99) received the B.E. and M.E. degrees in electronic engineering, and the Ph.D degree in information and communication engineering, all from the University of Tokyo, Tokyo, Japan, in 1994, 1996, and 1999, respectively.

He is currently with the Institute of Industrial Science, University of Tokyo, Tokyo, Japan, as a Postdoctoral Fellow. His current interests include coding theory, coded modulation, communication theory, and cryptography.

Dr. Isaka is a member of the IEICE.

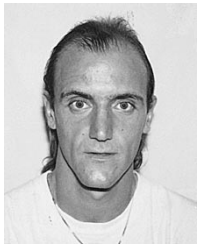

Marc P. C. Fossorier (S'90–M'95) was born in Annemasse, France, on March 8, 1964. He received the B.E. degree from the National Institute of Applied Sciences (INSA), Lyon, France, in 1987, and the M.S. and Ph.D. degrees from the University of Hawaii at Manoa, Honolulu, in 1991 and 1994, respectively, all in electrical engineering.

In 1996, he joined the Faculty of the University of Hawaii, Honolulu, as an Assistant Professor of Electrical Engineering. He was promoted to Associate Professor in 1999. His research interests include decoding techniques for linear codes, communication algorithms, combining coding and equalization for ISI channels, magnetic recording, and statistics. He co-authored (with S. Lin, T. Kasami, and T. Fujiwara) the book, *Trellises and Trellis-Based Decoding Algorithms* (Norwell, MA: Kluwer, 1998).

Dr. Fossorier was a recipient of a 1998 National Science Foundation Career Development Award. He has served as Editor for the IEEE TRANSACTIONS ON COMMUNICATIONS since 1996, as Editor for the IEEE Communications Letters since 1999, and he is currently the Treasurer of the IEEE Information Theory Society.

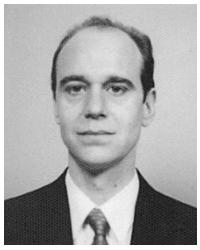

Robert H. Morelos-Zaragoza (S'83–M'89–SM'98) was born in Houma, LA. He received the B.S. and M.S. degrees in electrical engineering from the National Autonomous University of Mexico, Mexico City, in 1985 and 1987, respectively, and the Ph.D. degree in electrical engineering from the University of Hawaii at Manoa, in 1992.

From August 1992 to March 1993, he was an Assistant Professor at the Center of Telecommunications of the Instituto Tecnológico y de Estudios Superiores de Monterrey, Monterrey, NL, México. From 1993 to 1994, he was a Visiting Research Associate at the Department of Information and Computer Science, Osaka University, Osaka, Japan. From 1994 to 1995, he was a JSPS Postdoctoral Fellow at the Graduate School of Information Science, Advanced Institute of Science and Technology, Nara, Japan. From March 1995 to June 1997, he was a Research Associate at the Institute of Industrial Science, the University of Tokyo, Tokyo, Japan. From June 1997 to July 1999, he was with the Channel Coding Group of LSI Logic Corporation, Milpitas, CA. Since August 1999, he has been a researcher with the Advanced Telecommunications Laboratory, SONY Computer Science Laboratories, Inc., Tokyo, Japan. His research interests include error control coding, coded modulation, and design of digital communications systems.

Dr. Morelos-Zaragoza is a member of Eta Kappa Nu and the Institute of Electronics, Information and Communication Engineers (IEICE) of Japan.

Shu Lin (S'62–M'65–SM'78–F'80) received the B.S.E.E degree from the National Taiwan University, Taipei, Taiwan, R.O.C., in 1959, and the M.S. and Ph.D. degrees in electrical engineering from Rice University, Houston, TX, in 1964 and 1965, respectively.

In 1965, he joined the Faculty of the University of Hawaii, Honolulu, as an Assistant Professor of Electrical Engineering. He was promoted to Associate Professor in 1969, and to Professor in 1973. In 1986, he joined Texas A&M University, College Station, as the Irma Runyon Chair Professor of Electrical Engineering. In 1987, he returned to the University of Hawaii. From 1989 to 1995, he served as the Chairman of the Department of Electrical Engineering. He retired from the University of Hawaii in 1999 and joined the University of California at Davis, where he is now a Visiting Professor. He spent 1978–1979 as a Visiting Scientist at the IBM Thomas J. Watson Research Center, Yorktown Heights, NY, where he worked on error control protocols for data communication systems. He spent the academic year of 1996–1997 as a Distinguished Visiting Professor at the Nara Advanced Institute of Science and Technology, Nara, Japan, and as a Visiting Chair Professor at the Technical University of Munich, Munich, Germany. He has published more than 100 technical papers in IEEE TRANSACTIONS and other prestigious refereed journals and more than 200 conference papers. He is the author of the book, *An Introduction to Error-Correcting Codes* (Englewood Cliff, NJ: Prentice-Hall, 1970). He co-authored (with D.J. Costello) the book, *Error Control Coding: Fundamentals and Applications* (Englewood Cliffs, NJ: Prentice-Hall, 1982), which has been widely adopted either as a text for a course in error control coding or as a reference for practicing communication engineers over the world for the last 17 years. He also co-authored (with T. Kasami, T. Fujiwara and M. Fossorier) the book, *Trellises and Trellis-Based Decoding Algorithms,* (Norwell, MA: Kluwer, 1998). He has contributed chapters for six other books. He has been awarded several patents. A convolutional code constructed by him in 1965 was used in NASA's Pioneer 9 solar orbit space mission, launched in 1968. He has served as the Principal Investigator on 25 research grants. His current research areas include algebraic coding theory, coded modulation, turbo coding, low-density parity-check codes, soft-decision decoding, error control systems, and satellite communications.

Dr. Lin is a member of the IEEE Information Theory Society and the IEEE Communications Society. In 1991, he was the President of the IEEE Information Theory Society. He served as the Associate Editor for Algebraic Coding Theory for the IEEE TRANSACTIONS ON INFORMATION THEORY from 1976 to 1978, and as Program Co-Chairman of the IEEE International Sysposium on Information Theory, held in Kobe, Japan, in June 1988. He also served as Co-Chairs for a number of IEEE Information Theory Workshops and a number of International Communication Conferences and Symposia. He was a recipient of the Alexander von Humboldt Research Prize for U.S. Senior Scientists in 1996 and the IEEE Third Millenium Medal for his outstanding contributions in error control coding and engineering education.

Hideki Imai (M'74–SM'88–F'92) was born in Shimane, Japan, on May 31, 1943. He received the B.E., M.E., and Ph.D. degrees in electrical engineering from the University of Tokyo, Tokyo, Japan, in 1966, 1968, and 1971, respectively.

From 1971 to 1992, he was on the faculty of Yokohama National University, Yokohama, Japan. In 1992 he joined the faculty of the University of Tokyo, where he is currently a Full Professor in the Institute of Industrial Science. His current research interests include information theory, coding theory, cryptography, spread-spectrum systems and their applications.

Dr. Imai was elected an IEEE Fellow for his contributions to the theory of coded modulation and two-dimensional codes in 1992. He has chaired several committees of scientific societies such as the IEICE Professional Group on Information Theory. He served as the editor for several scientific journals of IEICE, IEEE, etc. He has chaired many international conferences such as the 1993 IEEE Information Theory Workshop and 1994 International Symposium on Information Theory and Its Applications (ISITA'94). Dr. Imai has been on the Board of IEICE, the IEEE Information Theory Society, Japan Society of Security Management (JSSM), and the Society of Information Theory and Its Applications (SITA). He has served as President of the IEICE Engineering Sciences Society and SITA. He received Excellent Book Awards from IEICE in 1976 and 1991. He also received the Best Paper Award (Yonezawa Memorial Award) from IEICE in 1992, the Distinguished Services Award from the Association for Telecommunication Promotion Month in 1994, and the Telecom System Technology Prize from the Telecommunication Advancement Foundation and Achievement Award from IEICE in 1995. In 1998, he was awarded the Golden Jubilee Paper Award by the IEEE Information Theory Society.